FOAM, a new simple benthic degradative module for the LAMP3D model: an application to a Mediterranean fish farm

Patrizia De Gaetano [1], Andrea M. Doglioli [2], Marcello G. Magaldi [3], Paolo Vassallo [4], Mauro Fabiano [4]

[1] DIFI, Dipartimento di Fisica, Università di Genova

[2] Aix-Marseille Université ; CNRS ; LOB-UMR 6535, Laboratoire d'Océanographie et de Biogéochimie, OSU/Centre d'Océanologie de Marseille

[3] Rosenstiel School of Marine and Atmospheric Science (RSMAS), Division of Meteorology and Physical Oceanography (MPO), University of Miami

[4] DIPTERIS, Dipartimento per lo Studio del Territorio e delle sue Risorse, Università di Genova

Corresponding author address:

Patrizia De Gaetano, DIFI, Dipartimento di Fisica, Universitá di Genova, Via Dodecaneso 33, 16146 Genova, Italia.

Phone: +39 010 353 6385 Fax: +39 010 353 6354 E-mail: degaetano@fisica.unige.it

Running title: FOAM, Finite Organic Accumulation Module

Keywords: Biodegradation modeling, Aquaculture impact, Mediterranean Sea, Husbandry, Net-pen, Organic matter.

Preprint submitted to Aquaculture Research *March 11, 2008*

Abstract

The modeling framework already introduced by Doglioli et al. (2004a) to predict the potential impact of a marine fish farm is improved following different directions. Namely: (i) real historic current-meter data are used to force the simulations; (ii) settling velocity values specifically targeting Mediterranean fish species are used; and (iii) a new benthic degradative module, FOAM, is added to the modeling framework. FOAM uses the output of the other functional units of the modeling framework to calculate the organic load on the seabed. FOAM considers the natural capability of the seafloor in absorbing part of the organic load. Different remineralization rates reflect the sediment stress level according to the work of Findlay & Watling (1997).

Organic degradation for both uneaten feed and faeces is evaluated by changing release modality (continuous and periodical) and by varying the settling velocities. It is found that the maximum impact on the benthic community is observed either for quickly-sinking uneaten feed released twice a day, or for less intense near bottom current conditions. If both the above mentioned scenarios coexist, a high stress level is established in the sediment. The model also suggests that the use of self-feeders in cages can significantly reduce farm impacts. These results show how the new and more complete modeling framework presented here is able to improve the objectivity in the decision making processes and how it may be successfully used for planning and monitoring purposes.

1 Introduction

The increase in global fish consumption and the decrease of wild fish stocks are the main reasons behind the continuous development of marine aquaculture (FAO Fisheries Division, 2006, `http://www.fao.org/docrep/009/a0874e/a0874e00.htm`). The worldwide expansion of marine fish farms, however, has always been generating concern regarding the possible impacts on coastal ecosystems. Already in 1995, the Food and Agriculture Organization (FAO) of the United Nations adopted a Code of Conduct for Responsible Fisheries. The Code provided the necessary framework for national and international efforts to ensure sustainable exploitation of aquatic living resources. Particular attention was paid to the aquaculture growth in accord with the sustainable and integrated use of the environment, taking into account the fragility of coastal ecosystems, the finite nature of their natural resources and the needs of coastal communities. In 2001, following the same direction, the European Union started to set up a strategy for sustainable aquaculture development with the Biodiversity Action Plan for Fisheries (COM 162, 2001) and the European Strategy for Sustainable Development (COM 264, 2001). These two documents led to the more recent and specific Strategy for the Sustainable Development of European Aquaculture (COM 511, 2002).

Marine aquaculture operations are still very expensive, and the only means by which profitability can be sustained is to intensify fish production. Unfortunately this intensification increases the already existing concerns about reaching and surpassing the natural capability of the environment. The scientific literature has identified the main environmental impact from fish farms to be the release of particulate waste products (Hall et al., 1990; Holmer & Kristensen, 1992; Karakassis et al., 2000). The particulate wastes increase the organic load on the benthic environment and might determine changes in the community structure and in the biodiversity of the benthic assemblages (Tsutsumi et al., 1991; Wu et al., 1994; Vezzulli et al., 2002, 2003). Therefore we are in need for predictive tools able to assess whether or not the establishment of a new farm (or the permission for an increase in production of an already existing one), can result in a potential impact on the surrounding environment.

Numerical models can be used to perform environmental impact predictions and test different scenarios. The interest in tracking aquaculture wastes with mathematical models has been rapidly increasing in time as a consequence (Henderson et al., 2001). In the past we have moved from using analytical models describing oversimplified dispersion patterns in a constant flow in time and space (Gowen et al., 1989), to implementing equations with too many simplifying assumptions about hydrodynamics (Gillibrand & Turrell, 1997). Others have developed particle tracking models using hydrographic data and were therefore limited in their simulations by the sparse data in time and in space (Cromey et al., 2002). Ocean dynamics, instead, are usually very complex and ocean ecosystems are likely to experience current reversals and flow variability. Pioneering numerical studies used circulation models focusing on strongly tidally driven systems. In this case, the flow could have been considered obeying two-dimensional (2D) vertically averaged dynamics (Panchang et al., 1997; Dudley et al., 2000). Unfortunately, the 2D approximation can be inappropriate in more complex and dynamical systems where vertical phenomena affect the dispersion of different particles. Having this in mind, some of us were the first ones to directly take into account the three-dimensional (3D) ocean circulation and its variability in tracking different aquaculture wastes (Doglioli et al., 2004a). Nevertheless, to our knowledge, Doglioli et al. (2004a) (hereinafter referred to as DMVT04) still represents the only application of a 3D hydrodynamical model for aquaculture purposes.

The present study takes place following the continuous effort in improving the framework initially set up by DMVT04. The improvements and the assessment of their relative importance have been done mainly in three areas and represent the core and the original intent of this work. Namely, in this study we (a) improved our hydrodynamics using real historic current-meter data to force the simulations; (b) improved our dispersion using a larger number of particles and updating the settling velocity values specifically for Mediterranean fish species and for their feed; and (c) added a new coupled benthic module to consider the environmental response to the organic load from the cages.

In DMVT04 some of us used idealized winds to force simulations. The choice of the winds was based on a statistical treatment of 34 years of wind data and it allowed us to carry out a complete 12-day hydrodynamic simulation during which wind direction and speed were changing according to a typical local meteorological sequence. In a later paper, however, some of us successfully used historical current-meter data to study the hydrodynamic characteristics of the area under examination (Doglioli et al., 2004b). Since the focus of this study is to move toward a more realistic scenario, we decided to implement the already validated forcing setup used in Doglioli et al. (2004b). This mainly implies that the open boundary conditions and the forcing evaluation are improved by applying realistic current measurements.

On the other hand, settling velocity values for uneaten feed and faeces represent key parameters for aquaculture waste dispersion models. The lack of values specifically targeting Mediterranean fish and their feeds obliged DMVT04 to use the only values available in the literature, i.e. the ones measured for salmonids (Chen et al., 1999a,b). However, two recent works filled this important gap. On one side, some of us, in Vassallo et al. (2006) presented the settling velocities of a feed usually utilized in Mediterranean farms (the 'Marico Seabass and Seabream' pellets produced by Coppens International), while on the other side, Magill et al. (2006) measured the settling velocities of Gilthead Sea Bream and Sea Bass faecal particles collected in sediment cores in a Greek fish farm. A second original aspect of this study is that it uses these new values, paying particular attention to the role they play in the overall results.

Finally, we recognize that following only the fate of the particles as we did in

DMVT04 is not sufficient to correctly assess the organic load on the sea bottom. The modeling effort should consider the natural capability of the benthic environment in reacting and absorbing fluctuations in the organic load. Our model framework is integrated with an additional new numerical benthic degradative module, the Finite Organic Accumulation Module (FOAM). FOAM is mainly based on the ideas expressed in the work of Findlay & Watling (1997) (hereinafter referred to as FW97). They proposed an index of impact based on the ratio between the quantity of oxygen supplied to the sediment and the quantity of oxygen demanded by the sediment. **The oxygen supply is a function of the near bottom flow velocities and is calculated by the empirical relation put forth by FW97**. The oxygen demand is based on the organic load from the cages and it is strongly related to the microbial benthic metabolism rate. As pointed out by the same authors, the equations proposed by FW97 can be easily exploited by numerical modelers since the only needed input variables are the bottom flow velocities and the organic flux toward the seabed. Since our model does consider the vertical dimension, it is also able to provide these important required data. Furthermore, its intrinsic Lagrangian nature allows a simple numerical implementation of the ideas proposed in FW97.

The rest of this paper is organized as follows. In Section 2 a description of the study area and the details of the modeling effort are provided. The results of the numerical experiments are presented in Section 3 and discussed in Section 4. Finally the conclusions are given in Section 5.

2 Methods

The simulations are carried out for the offshore fish farm located in the Ligurian Sea already described in DMVT04 (Fig. 1). The sea cages are located at about 1.5 km from the coast and they cover an area of 0.2 km^2. The bottom depth ranges between 38 m and 41 m. The farm is composed of 8 fish cages with a capacity of 2000 m^3

each. The reared biomass is 20 kg m^{-3} for an annual mean production of about 200 ton $year^{-1}$. The fish in the cages are Gilthead Sea Bream (*Sparus aurata*) and Sea Bass (*Dicentrarchus labrax*).

The modeling framework consists of different models which are coupled together into a single functional unit (Fig. 2). The hydrodynamic model is the Princeton Ocean Model (POM) and it is used to derive space and time information of the circulation of the coastal area. POM is coupled online with the three-dimensional Lagrangian Assessment for Marine Pollution Model (LAMP3D). LAMP3D is used to track the particle positions in time and space. The Finite Organic Accumulation Model (FOAM) represents the biochemical component of the modeling system and it uses POM and LAMP3D outputs to estimate the potential environmental impact due to the organic load from the cages. POM and LAMP3D calculate the bottom velocities and the particle fluxes to the bottom and these values are then used by FOAM to calculate the final organic load in each mesh of its numerical domain.

The following part of this section gives a more detailed description of the entire modeling framework.

2.1 The advective and dispersive models: POM and LAMP3D

Some historical measurements of the coastal current in the area are available in terms of current-meter time series and hydrographic surveys, covering a total of 10 months during 1978 - 1979 (Astraldi & Manzella, 1983). Data are archived in the SIAM database (`http://estaxp.santateresa.enea.it/www/siams/prov102.html`), and they have been kindly provided to us by the Italian National Agency for New Technologies, Energy and Environment (ENEA) and the National Research Council (CNR). In this study, we concentrate on the winter-spring period, when the currents are stronger and better defined and the stratification is being formed. We select the period from February 8th 1979 to June 30th 1979 and we force the model on the eastern boundary. At the western boundary a radiation condition is imposed. The described setup is the same used and validated in Doglioli et al. (2004b). The reader is referred to this paper for a more detailed description of the boundary conditions and for their validation. Here, complete four-month simulations are carried out, obtaining current data necessary for the dispersion-degradation runs. The first velocity value ($U = -0.19$ m s^{-1}), measured on February 8th 1979, is provided on the whole domain as an initial condition for all the simulations. Since the objective of this work is simulating longer time periods, we cyclically repeat the real current-meter data as boundary conditions to force the runs. Consequently, the organic matter accumulation on the seabed can be estimated for longer time periods and the dependence of the model results on the initial condition can be reduced.

Moreover, since the primary focus of this study is the organic load on the seafloor and not the fate of the dissolved nutrients, we adopt a new setup with respect to that used in DMVT04 for the hydrodynamical model POM and the dispersive model LAMP3D (see Fig. 1). The POM grid has 115 $\times$ 80 meshes with a spatial resolution of 400 m along the x-direction and 200 m along the y-direction. **This resolution reflects the best available bathymetric data in the area**. The LAMP3D numerical domain, instead, is smaller (8 km $\times$ 4 km), and it is nested in the POM grid with the same spatial resolution (400 m$\times$ 200 m).

The other dispersive parameters are unchanged with respect to DMVT04, with the exception of the Lagrangian particle number that was increased to 620000 for greater precision and better rendering. The DMVT04's assumptions on the organic carbon concentration in feed and faecal waste are adopted. In particular, the value of 5% for the feed loss was recently confirmed by results of MERAMED project (`http://www.meramed.com`). Nevertheless, since the number of particles is increased with respect to DMVT04, we calculate new conversion factors for uneaten feed and faecal waste (Table 1). We also keep calculating nitrogen loading rates for validation purposes (see Section 3) using the same conversion factors used in DMVT04 for nitrogen.

The lack of data for Mediterranean species obliged us in DMVT04 to use the values proposed by Chen et al. (1999a) and Chen et al. (1999b) for salmonids. Recently Magill et al. (2006) have measured the settling rates of faecal material of Gilthead Sea Bream and Sea Bass, while, under laboratory conditions reproducing the Mediterranean sea water, Vassallo et al. (2006) have provided the settling velocity values of a typical growing sequence of feed pellets for the same species. We therefore used the values of these recent works in our simulations.

All the parameters used in the hydrodynamic and dispersive models are summarized in the upper part of Table 1, while the different settling velocity values are reported in Table 2.

2.2 The benthic module: FOAM

A new bottom boundary condition is implemented in our model. When a numerical particle touches the seabed, it is considered as biodegradable settled matter and it is treated by the benthic module FOAM. FOAM covers the same area of the dispersive model but its resolution is 10 times higher, namely 40 m$\times$ 20 m (Fig. 1). **This resolution adequately represents the known processes of degradation and is acceptable in terms of computational time. In the case of FOAM, a higher resolution is feasible because its calculations are performed offline.**

According to FW97, the organic accumulation on the bottom leads to different rates of mineralization in relation to the level of stress the seabed is exposed to. In order to simulate the biological reaction of the microbial benthic community to the variations in the organic enrichment, we assign the status of the sediment in each grid mesh according to the ratio between the benthic oxygen supply and the demand.

In FOAM the same equations and constants proposed by FW97 are used. The oxygen supply is a function of the near bottom velocities and can be calculated by simple Fickian diffusion arguments and expressed by the empirical relation

$$\mathrm{O}_2^{sup} \ = \ A \ + \ B \cdot \log(\overline{v}) \tag{1}$$

where A and B are constants (see Table 1) and $\overline{v}$ is a time averaged current velocity taken at 1 m from the bottom. It is important to note that $\overline{v}$ is just the numerical value of the bottom flow velocity when it is expressed in cm s^{-1}. In our model this value is obtained by linear interpolation of the velocity in the deepest vertical grid cell and by using an average time interval of $\Delta t = 2$ hours. This choice was already made by FW97 to describe oxygen supply to the benthos. Moreover, this time interval seems to be critical, since a 2 hour exposure to reduced oxygen and elevated hydrogen sulfide concentrations causes permanent damage to the gill tissues of sensitive infauna (Theede et al., 1969). The same choice of $\Delta t = 2$ hours is also supported by the more recent work by Morrisey et al. (2000).

The oxygen demand, instead, is a function of the organic carbon flux toward the sea bottom Flx^{Bot} according to the relation

$$\mathrm{O}_2^{dem} \ = \ C \cdot Flx^{Bot} \ + \ D \tag{2}$$

where, again, C and D are just constants (Table 1; **for more details refer to Fig. 2 and Fig. 3 in FW97**). If i and j are the grid mesh indexes in the x and y directions respectively, the carbon flux Flx^{Bot} in each grid mesh (i, j) at the instant k is calculated on the basis of the number of particles reaching the bottom, $n_{i,j}^{Bot}$, during an integration time interval dt, i.e.

$$Flx_k^{Bot} = \frac{n_{i,j}^{Bot} \cdot w^C}{dt \cdot \Delta x \cdot \Delta y} \tag{3}$$

In the equation (3), Δx and Δy are the horizontal grid sizes while w^C stands for the adopted organic carbon conversion factor. w^C varies if we consider feed or faeces and the different values are listed in Table 1.

Once the model provides O_2^{sup} and O_2^{dem} for each grid mesh, we can calculate the index of impact I as suggested by FW97 as

$$I_{i,j} = \frac{O_2^{sup}}{O_2^{dem}} \tag{4}$$

Based on I we can identify three different levels of stress: non-stressed sediments, intermediately-stressed sediments and highly-stressed sediments. FW97 suggested that when $I > 1$, the supply of oxygen is in excess of the demand and therefore the impact is minimal. When $I \approx 1$ the impact can be moderate while when $I < 1$, the sediment exhibits the azoic sediment endpoint and the resulting impact is high. In our model the discrete FW97 criterion for the different levels becomes

· no stress, if $I_{i,j} > 1 + \Delta_{fw}$;

· medium stress, if $(1 - \Delta_{fw}) \leq I_{i,j} \leq (1 + \Delta_{fw})$;

· high stress, if $I_{i,j} < 1 - \Delta_{fw}$.

Sensitivity tests on the Δ_{fw} parameter are performed in a range varying from $\Delta_{fw} = 0.05$ to $\Delta_{fw} = 0.5$. We observe no meaningful differences, so, for precautionary reasons, the value of $\Delta_{fw} = 0.5$ is adopted.

When the level of stress is decided according to the value $I_{i,j}$, different rates of mineralization are used in each grid mesh. In our code, this is obtained by subtracting different quantities to the already calculated organic carbon concentration fluxes. The subtracted amounts are the same as FW97 and are shown in the lower part of Table 1. On the basis of the obtained fluxes, the organic carbon concentration $Conc^{Bot}$ in each grid mesh (i, j) is calculated as

$$Conc^{Bot} = \sum_{k=1}^{NT} Flx_k^{Bot} \cdot dt \tag{5}$$

where NT is the number of the time intervals of the simulation.

All the parameters used in the benthic module are summarized in the lower part of Table 1.

3 Results

The modeled water circulation is in agreement with the past literature in the area: the simulations show the presence of the observed westward transport (Astraldi & Manzella, 1983; Astraldi et al., 1990), persisting for almost the entire simulated period (winter-spring). The obtained general circulation also agrees with other numerical experiments such as Baldi et al. (1997) and DMVT04. It is also possible to observe current separation and eddy formation behind the Portofino Promontory as in Doglioli et al. (2004b). For a more quantitative hydrodynamic validation, we use the same approach as in DMVT04. Current data simulated by the model are compared with data collected by one current meter, C1, located at 2 km to the west of the farm. Current speed and direction were sampled every hour at 20-m depth from February 1993 to March 1994. Table 3 shows current data from C1 and the model outputs. When we use only one cycle at the eastern boundary and we prescribe the first velocity value on the whole domain as an initial condition, the seasonal averages from the observations are systematically lower than the model ones (see values for the first cycle). When we cyclically repeat the boundary conditions to force the runs and we use as the initial condition the last velocity field of the previous cycle, the comparison with the C1 data improves (see values for the fifth cycle). We speculate that the larger discrepancy observed in the first cycle is due to the artificial highly energetic initial condition. Therefore, we decide to run five cycles of linked simulations and we subsequently neglect the first two in order to reduce the sensitivity to the initial conditions. The three linked cycles account for a total of 430 simulated days and their averages are also reported in Tab. 3. In this case, the data are very close to the values calculated by the model. Current direction agrees with the observed along-shore water movement. Sporadic current reversals are also simulated thanks to the inversions of the direction of the velocity at the inflow boundary condition.

At the same time, we can use sediment observations around the cages to validate our dispersive runs. A Van Veen grab was used to collect sediment samples in three repetitions in each of the four stations surrounding the fish farm (**see Fig.7 of DMVT04 for the exact location of the sampling stations**). With respect to DMVT04, additional recent data were collected in the same stations. All the samples were analyzed for total nitrogen and total phosphorus. The comparison between absolute values of these data and the model outputs is not possible since, in order to express both of them in the same units, we would need to make strong assumptions on the sediment density as well as on the sampling methodology. We therefore use the same approach used in DMVT04. Fig. 3 shows the agreement between the field and modeled data. In particular, field sediment nutrients are highest in station S2 and lowest in station S4, which agrees with model output for total nitrogen under westward transport. To facilitate the comparison of results for the reader, in the same Fig. 3, we also show the performance of the old setup adopted in DMVT04 and the field data as they were at that time.

The above comparison with the only data available in the area, allows us to focus on the dispersion model and on the benthic modeled impact. The time series of the dispersion model output are also referred to the three last cycles of linked simulations. In order to explore the differences in the runs by varying waste typology, release condition and settling velocity, we set up the following experiments:

A1) slowly sinking feed in continuous release;

A2) quickly sinking feed in continuous release;

B1) slowly sinking feed in periodical release;

B2) quickly sinking feed in periodical release;

C1) slowly sinking faeces (continuous release);

C2) quickly sinking faeces (continuous release).

Note that for periodical release we mean that the feed is supplied twice a day, and slowly and quickly sinking are referred to the minimum and maximum values listed in Table 2 for the two different waste typologies. In Table 2 the slowly sinking values are indicated with a single arrow pointing toward the bottom (↓), while the quickly sinking values with a double one (⇓).

Results from the benthic module are presented in relation to (i) the extension of the impacted area, (ii) the position of this area in terms of its barycenter, (iii) the benthic trophic conditions and (iv) the predicted organic concentration at the barycenter. The choice of these parameters allows the simple and objective estimation of the degree and the location of the potential impact.

The impacted surface S is the sum of the areas of the grid meshes where particles are still present even after the benthic degradation activity. The position of the barycenter (x_b, y_b) of this area is basically a position weighted by the number of particles left in each cell after the degradation. It is simply expressed as

$$x_b = \frac{\sum_{j=1}^{N} \sum_{i=1}^{M} i \cdot n_{i,j}^{left}}{n_{Tot}^{left}} \tag{6}$$

$$y_b = \frac{\sum_{j=1}^{N} \sum_{i=1}^{M} j \cdot n_{i,j}^{left}}{n_{Tot}^{left}} \tag{7}$$

where M and N are the numbers of meshes in the x and y directions, $n_{i,j}^{left}$ is the number of particles left on the bottom in the mesh (i, j) and $n_{Tot}^{left} = \sum_{j=1}^{N} \sum_{i=1}^{M} n_{i,j}^{left}$ is the total number of particles left on the bottom after the degradation. The benthic trophic condition and the predicted organic concentration at the barycenter are simply given by the parameter I and $Conc^{Bot}$ in the grid mesh corresponding to the barycenter position.

We initially describe the effects on the extension of the impacted area. Fig. 4 shows the time series of the calculated extensions in the different experiments and the temporal variations of the modeled current velocity near the cages (Fig. 4D). The slowly sinking feed particles continuously released (Fig. 4A, solid black line) are dispersed by the current a little bit more than the quickly sinking ones (dashed gray line). This is also confirmed by the time averages and the standard deviations for the experiments A1 and A2 (see Table 4). The situation changes when we consider periodical release (Fig. 4B). In this case both slowly and quickly sinking particles are dispersed on a larger area than in the continuous case. However, while for slowly sinking particles this area is much larger and less variable in time than in the continuous release, for quickly sinking ones, the area is just a little bit bigger and more variable (see Table 4). The variability of the dispersion is therefore associated with the current velocity and it increases both with periodical release and with decreasing settling velocity values. For faecal pellets (Fig. 4C), the impacted area is smaller than in the previous cases. Moreover, faecal wastes show greater time variability than the uneaten feed, no matter what the feed release is. The slowly sinking faecal particles impact smaller areas with respect to the quickly sinking ones, and also the variability is smaller than the quickly sinking ones (Table 4).

Fig. 5 gives a better visualization of what has been stated so far and, at the same time, it shows the position of the barycenter of the impacted area. In this figure, we schematize the extension of the impacted area with a circle centered in the barycenter and having an area equivalent to the one already calculated. The gray scale represents the time evolution of the results every sixty days, while a circle is drawn every ten days. In the case of feed, for both continuous and periodical releases, the barycenter of the impacted area is found at approximately 25 m southwestward from cages. For the same simulations, a less significant time variability is observed (Fig. 5A1, A2, B1 and B2) and this means that the impacted area is always larger and that higher stress levels are expected. In the case of faecal wastes, instead, the barycenter shows greater time variability, according to changes in current direction and intensity (Fig. 5C1 and C2). This variability results in a dispersion of the faecal particles in different areas and therefore lower stress levels are expected.

To better emphasize these results, we can look at the scatter diagram of the parameter I at the barycenter position in time (Fig. 6). For clarity, all values greater than 2 are artificially assigned to 2 in this figure. For feed particles continuously released (Fig. 6A), I mainly stays in the non-stressed range (i.e. $I > 1.5$), sometimes goes up to the intermediately-stressed range, but the highly-stressed level is rarely reached. There is a slight tendency for quickly sinking particles to stay more in the intermediate regime than the slow ones (Table 4). For periodical release (Fig. 6B), I is often in the non-stressed range, very rarely in the intermediately-stressed range but it reaches the highly-stressed level more frequently than before. An easy and quick check shows that the highly-stressed values are registered, in this case, in the period going from 2 to 4 hours after the release. No significant difference can be observed between slowly and quickly sinking particles. For faecal wastes (Fig. 6C), the parameter I is practically always greater than 2 (for this reason in the plot all dots are squeezed in the top) for both slowly and quickly sinking particles.

Finally, the mean values of the computed organic matter concentration $Conc^{Bot}$ remaining on the seabed at the barycenter position after the degradation are reported in the last column of Table 4. The organic carbon amount due to feed waste almost linearly increases with time and the maximum values are reached in the case of the most quickly sinking feed particles in periodical release. The faecal waste instead seems to be completely degraded and it does not contribute to organic carbon concentration at the bottom.

All the results are summarized in Table 4.

4 Discussion

The new model setup is shown to better reproduce both the hydrodynamics and the dispersion in the investigated area. This is mainly due to the new forcing which is based on current meter data and leads to more realistic results. As already remarked in previous works, current direction and intensity strongly influence the position of the impacted area and the degradation of the settled matter (FW97, Morrisey et al., 2000). Nevertheless, the processes involved are strongly non-linear and it is difficult to assess the role played by each parameter in the model.

When particles sink relatively quickly (settling velocities are one order of magnitude less than the current velocity, as a lower limit) the impacted area does not vary and the barycenter position depends on the main direction of the current. Instead, for relatively slowly sinking particles, the variability of the current starts to play a major role. This different behavior explains why the barycenter of the uneaten feed remains practically motionless, while the one for the faeces is very mobile.

At the same time, current intensity reduces bottom degradation thanks to two different processes. On one hand, a stronger current brings more oxygen to the sediment and makes degradation more efficient. On the other hand, the same stronger current increases waste dispersion resulting in a wider impacted area and in lower waste concentrations on the bottom. Faeces do not contain much organic carbon and the strong degradation is able to remove almost all the settled matter. Uneaten feed contains more organic carbon and sinks more rapidly than faeces. As a result, much more carbon accumulates on the sea floor and it is only partially degradated even in presence of strong currents. This also explains the observed small variability of the size and position of the impacted area.

Since we use the settling velocity values for faeces measured by Magill et al. (2006), it is particularly interesting to compare our results with theirs. In order to do this, we calculated the accumulation rates in the barycenter for different sinking faeces. We obtained values of 11 g faeces m^{-2} year^{-1} and 19 g faeces m^{-2} year^{-1} for slowly and quickly sinking particles, respectively. These values are about two orders of magnitude smaller than the ones reported in Magill et al. (2006). Two arguments can be provided to explain this discrepancy. Firstly, the total fish biomass in the cages is not reported in Magill et al. (2006) and this does not allow for a correct quantitative comparison. The policy of the fish farm studied in this work is to keep low biomass per cage (Roberto Co', AQUA s.r.l., personal communication). It is likely that the Greek fish farm studied by Magill et al. (2006) has a high biomass value per cage. Secondly, with the new module FOAM, we introduced the degradation of the settled organic carbon which is not considered instead by Magill et al. (2006). However, since we adopted the degradation rates proposed by FW97 for Atlantic fish farm, it is also possible that these values are too high with respect to the Mediterranean ones. Unfortunately, to the best of our knowledge no value is available in literature to check if this is really the case. On the other hand, our results agree with the work of Magill et al. (2006) in predicting a greater impact for the faeces of *D. Labrax* respect to *S. Aurata*'s ones. The same results also agree with previous studies and confirm the uneaten feed to be the primary cause of ecological impact on the benthos community (Beveridge et al., 1991; Vezzulli et al., 2003). For this reason, we studied in more detail the feed release conditions. We found that a release occurring twice a day results in i) more frequent conditions of highly-stressed sediments and ii) larger impacted areas than a continuous release. These results support the idea already proposed in previous studies of using self-feeders to reduce the uneaten feed loss without affecting fish growth rates (Azzaydi et al., 1998, and references therein).

5 Conclusions

Aquaculture is the food-related activity with the most rapid growth in the world. Since this growth produces an immediate concern, it is necessary to develop tools to predict the environmental impacts coming from intensive marine fish farms.

In this study we improved the capability of the POM-LAMP3D model already proposed in a previous work (Doglioli et al., 2004a). We developed both a more realistic advection-dispersion setup and a new benthic model, the Finite Organic Accumulation Module (FOAM). Using the empirical relations put forth by Findlay &

Watling (1997), FOAM calculates the organic carbon degradation for three different levels of sediment stress. We performed several runs to simulate different scenarios by varying waste typology (faecal or feed), settling velocity of particles (on the basis of feed dimensions, fish size and reared species) and release conditions of feed (periodical or continuous). **At the same time, the same runs allowed us to test the stability of the model which appears very satisfactory.**

We obtained more satisfactory results for the hydrodynamics and dispersion than in Doglioli et al. (2004a). Moreover, FOAM revealed its ability to simulate different scenarios by switching suitable parameters.

The results presented in relation to the extension of the impacted area and the position of its barycenter show that the continuously released feed settles within a narrow area near the cages (impact area maximum 6500 m^2; barycenter shifting amplitude 10 m; cages maximum distance 25 m); while the feed released twice a day spreads on a larger area centered near the cages (maximum area 8500 m^2; barycenter shifting amplitude 15 m; cages maximum distance 25 m). Faecal pellets accumulate on a smaller area within a greater and more variable range from the cages (maximum area 4000 m^2; barycenter shifting amplitude 100 m; cages maximum distance more than 50 m) with respect to uneaten feed. Maximum impacts, in terms of both stress parameter I and organic carbon concentration are due to the quickly settling feed, released in periodical mode and during slow current periods. Some mitigation of the impact is observed if feed is continuously released. The use of self-feeders has therefore been suggested to the farmers.

Further investigations may be necessary to verify the impact of combined feed and faeces settling, while mineralization rates for Mediterranean conditions and validation with specific in-situ measurements are required.

Acknowledgements

The authors warmly thank Roberto Festa for his useful advices and Corrado Ratto for his assistance and his interest in our research. More thanks to the Physics of the Atmosphere and Ocean Group of Genoa for the its support. We also thank Maurizio Costa for the environmental data and Roberto Co' and the staff of AQUA s.r.l. for their collaboration. We also thank Mandy Karnauskas for her helpful criticism and for revising the final version of the manuscript. CINFAI (National Consortium of Italian Universities for Physics of Atmospheres and Hydrosphere) is gratefully acknowledged to support the activities of the Physics of the Atmosphere and Ocean Group - Department of Physics - University of Genoa (Italy). We finally thank the anonymous Reviewer for the constructive criticism and support to the original manuscript.

References

Astraldi, M. & Manzella, G. (1983). Some observations on current measurements on the East Ligurian Shelf, Mediterranean Sea. *Cont. Shelf Res.*, 2:183–193.

Astraldi, M., Gasparini, G. & Manzella, G. (1990). Temporal variability of currents in the Eastern Ligurian Sea. *J. Goephys. Res.*, 95(C2):1515–1522.

Azzaydi, M., Madrid, J.A., Zamora, S., Snchez-Vzquez, F.J. & Martnez, F.J. (1998). Effect of three feeding strategies (automatic, ad *libitum* demand-feeding and time-restricted demand-feeding) on feeding rhythms and growth in European sea bass (*Dicentrarchus labrax*, L.). *Aquaculture*, 163:285–296.

Baldi, A., Marri, P. & Schirone, A. (1997). Applicazione di un modello per la simulazione del trasporto e della diluizione di inquinanti nelle acque costiere. Tech. rep. ENEA, RTI/AMB/GEM-MAR/97/04/RL2/A1.4.

Beveridge, M., Phillips, M., & Clarke, R. (1991). A quantitative and qualitative assessment of wastes from aquatic animal production. In Brune, D.E. & Tomasso, J.R., editors, Advances in World Aquaculture Volume 3, pages 506–533. World Aquaculture Society, Baton-Rouge, USA.

Chen, Y., Beveridge, M., & Telfer, T. (1999a). Physical characteristics of commercial pelleted atlantic salmon feeds and consideration of implications for modeling of waste dispersion through sedimentation. *Acquacult. Int.*, 7:89–100.

Chen, Y., Beveridge, M., & Telfer, T. (1999b). Settling rate characteristics and nutrient content of the faeces of Atlantic salmon, *Salmo salar* L., and the implications for modelling of solid waste dispersion. *Acquac. Res.*, 30:395–398.

Commission of the European Communities, Brussels (2001). Biodiversity action plan for fisheries. COM (2001) 162.

Commission of the European Communities, Brussels (2001). A Sustainable Europe for a Better World: A European Union Strategy for Sustainable Development. COM (2001) 264.

Commission of the European Communities, Brussels (2002). A Strategy for the sustainable development of European aquaculture Strategy for Sustainable Development. COM (2002) 511.

Cromey, C., Nickell, T., & Black, K. (2002). DEPOMOD-modelling the deposition and the biological effects of wastes solids from marine cage farms. *Aquaculture*, 214(1-4):211–239.

Doglioli, A.M., Magaldi, M.G., Vezzulli, L., & Tucci, S. (2004a). Development of a numerical model to study the dispersion of wastes coming from a marine fish farm in the Ligurian Sea (Western Mediterranean). *Aquaculture*, 231(1-4):215–235

Doglioli, A.M., Griffa, A., & Magaldi, M.G. (2004b). Numerical study of a coastal current on a steep slope in presence of a cape: The case of the Promontorio di Portofino. *J. Geophys. Res.*, 109, C12033, doi: 10.1029/2004JC002422

Dudley, R., Panchang, V., & Newell, C. (2000). Application of a comprehensive modeling strategy for the management of net-pen aquaculture waste transport. *Aquaculture*, 187:319–349.

Findlay, R. & Watling, L. (1997). Prediction of benthic impact for salmon netpens based on the balance of benthic oxygen supply and demand. *Mar. Ecol. Prog. Ser.*, 155:147–157

Gillibrand, P. & Turrell, W. (1997). The use of simple models in the regulation of the impact of fish farms on water quality in Scottish sea lochs. *Aquaculture*, 159:33–46.

Gowen, R., Bradbury, N., & Brown, J. (1989). The use of simple models in assessing two of the interactions between fish farming and marine environment. In DePauw, N., Jaspers, E., Ackefors, H., & Wilkins, N., editors, *Aquaculture - A Biotechnology in Progress*, pages 1071–1080. European Aquaculture Society.

Hall, P.O.J., Anderson, L.G., Holby, O., Kollberg, S. & Samuelsson, M. (1990) Chemical fluxes and mass balances in a marine fish cage farm. I. Carbon. *Mar. Ecol. Prog. Ser.*, 61:61–73

Henderson, A., Gamito, S., Karakassis, I., Pederson, P.& Smaal, A. (2001). Use of hydrodynamic and benthic models for managing environmental impacts of marine aquaculture. *J. Appl. Ichthyol.*, 17:163-172.

Holmer, M. & Kristensen, E. (1992) Impact of marine fish cage farming on sediment metabolism and sulfate reduction of underlying sediments. *Mar. Ecol. Prog. Ser.*, 80:191–201

Karakassis, I., Tsapakis, M., Hatziyanni, E., Papadopoulou, K., & Plaiti, W. (2000). Impact of cage farming of fish on the seabed in three Mediterranean coastal areas. *ICES J. Mar. Sci.*, 57(5):1462–1471.

Magill, S.H., Thetmeyer, H. & Cromey, C.J. (2006) Settling velocity of faecal pellets of gilthead sea bream (Sparus aurata L.) and sea bass (Dicentrarchus labrax L.) and sensitivity analysis using measured data in a deposition model. *Aquaculture*, 251(2-4):295–305

Morrisey, D.J., Gibbs, M.M., Pickmere, S.E. & Cole, R.G. (2000) Predicting impacts and recovery of marine-farm sites in Stewart Island, New Zealand, from the Findlay-Watling model. *Aquaculture*, 185:257–271

Panchang, V., Cheng, G., & Newell, C. (1997). Modeling hydrodynamics and aquaculture waste transport in Coastal Maine. *Estuaries*, 20:14–41.

Theede, H. , Ponat, A., Hiroki, K. & Schlieper., C. (1969). Studies on the resistance of marine bottom invertebrates to oxygen-deficiency and hydrogen sulphide. *Mar. Biol.*, 2:325-337.

Tsutsumi, H., Kikuchi, T., Tanaka, M., Higashi, T., Imasaka, K. & Miyazaki, M. (1991). Benthic faunal succession in a cove organically polluted by fish farming *Marine Pollution Bulletin*, 23:233–238

Vassallo, P., Doglioli, A.M., Rinaldi, F., & Beiso, I. (2006). Determination of physical behaviour of feed pellets in Mediterranean water *Aquac. Res.*, 37(2):119–126

Vezzulli, L., Chelossi, E., Riccardi, G. & Fabiano, M. (2002). Bacterial community structure and activity in fish farm sediment of the Ligurian Sea (Western Mediterrenean). *Aquacult. Int.*, 10(2):123–141.

Vezzulli, L., Marrale, D., Moreno, M., & Fabiano, M. (2003). Sediment organic matter and meiofauna community response to long-term fish-farm impact in the Ligurian Sea (Western Mediterranean). *Chem. Ecol.*, 19(6):431–440.

Wu, R., Lam, K., MacKay, D.W., Lau, T.C. & Yam, V. (1994). Impact of marine fish farming on water quality and bottom sediment: a case study in the sub tropical environment. *Marine Environmental Research*, 38:115–145

List of Figures

List of Tables

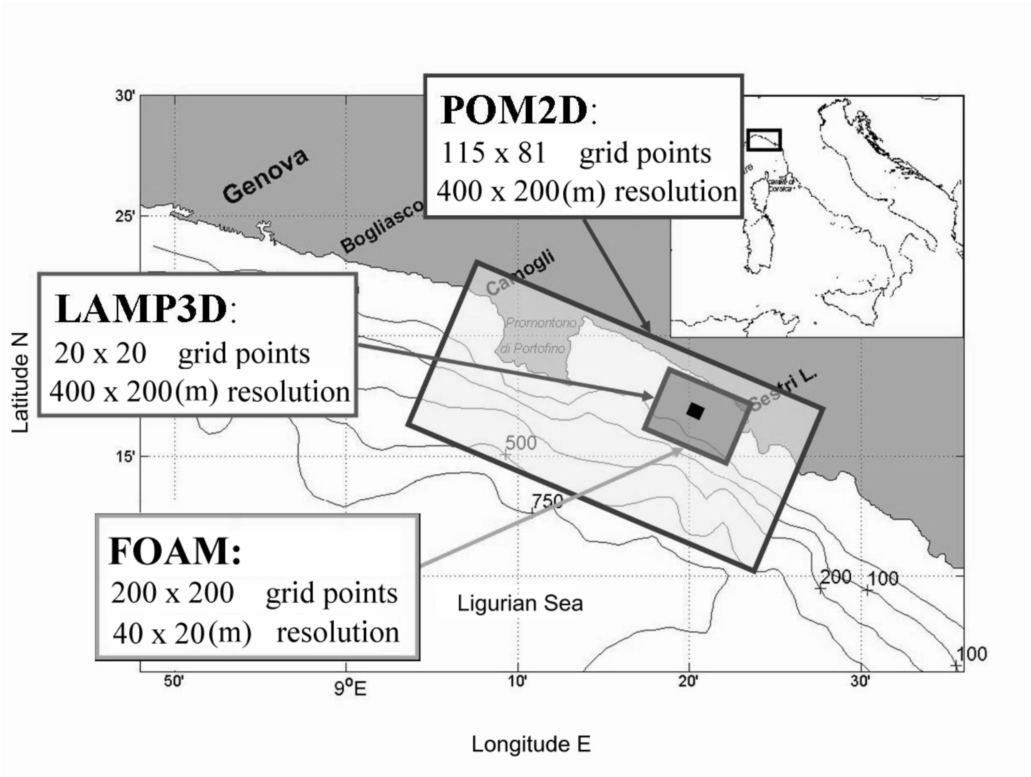
POM2D:
115 x 81 grid points
400 x 200(m) resolution
LAMP3D:
20 x 20 grid points
400 x 200(m) resolution
FOAM:
200 x 200 grid points
40 x 20(m) resolution
Genova
Bogliasco
Camogli
Promontorio di Portofino
Sestri L.
Ligurian Sea
500
750
200
100
100
30'
25'
15'
50'
9°E
10'
20'
30'
Latitude N
Longitude E

Figure 1:

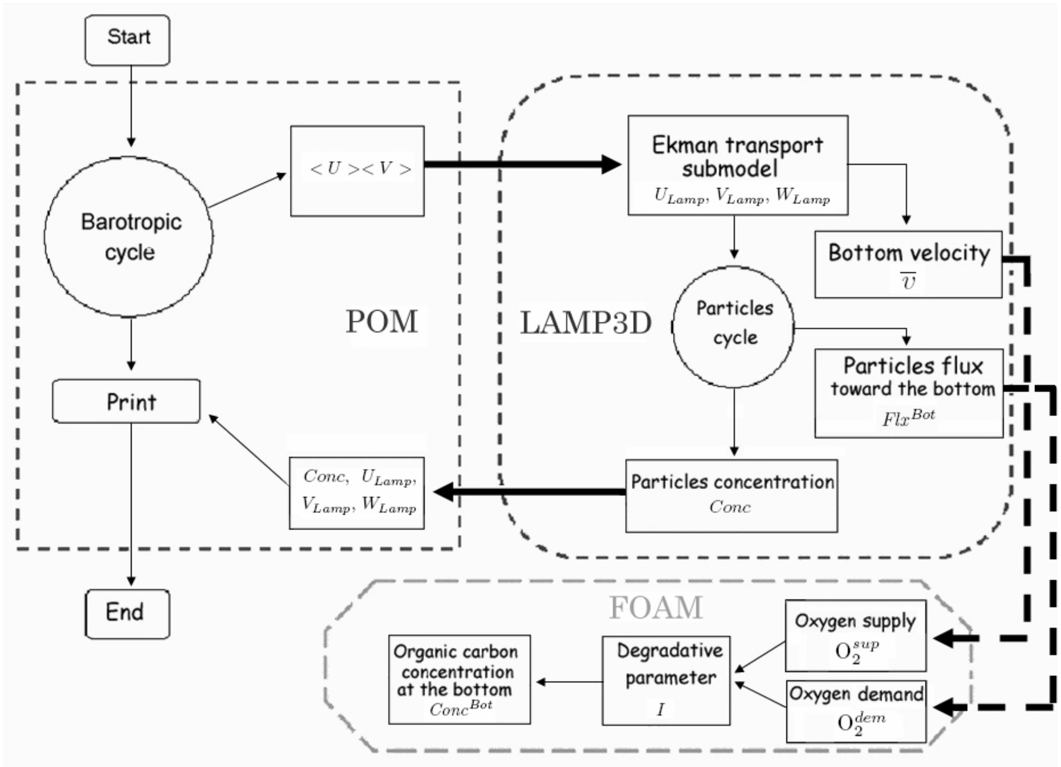

Start
Barotropic cycle
$<U><V>$
POM
Print
$Conc,\ U_{Lamp},$
V_{Lamp}, W_{Lamp}
End
Ekman transport submodel
$U_{Lamp}, V_{Lamp}, W_{Lamp}$
Bottom velocity
$\overline{v}$
LAMP3D
Particles cycle
Particles flux toward the bottom
Flx^{Bot}
Particles concentration
$Conc$
FOAM
Oxygen supply
O_2^{sup}
Oxygen demand
O_2^{dem}
Degradative parameter
I
Organic carbon concentration at the bottom
$Conc^{Bot}$

Figure 2:

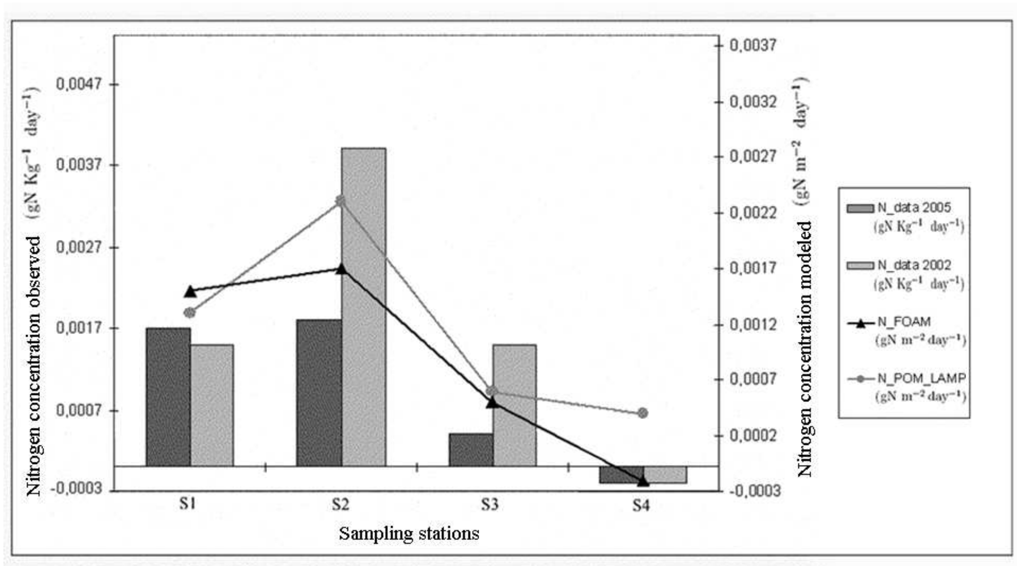
Nitrogen concentration observed (gN Kg^{-1} day^{-1})
Nitrogen concentration modeled (gN m^{-2} day^{-1})
0,0047
0,0037
0,0027
0,0017
0,0007
-0,0003
0,0037
0,0032
0,0027
0,0022
0,0017
0,0012
0,0007
0,0002
-0,0003
S1
S2
S3
S4
Sampling stations
N_data 2005 (gN Kg^{-1} day^{-1})
N_data 2002 (gN Kg^{-1} day^{-1})
N_FOAM (gN m^{-2} day^{-1})
N_POM_LAMP (gN m^{-2} day^{-1})

Figure 3:

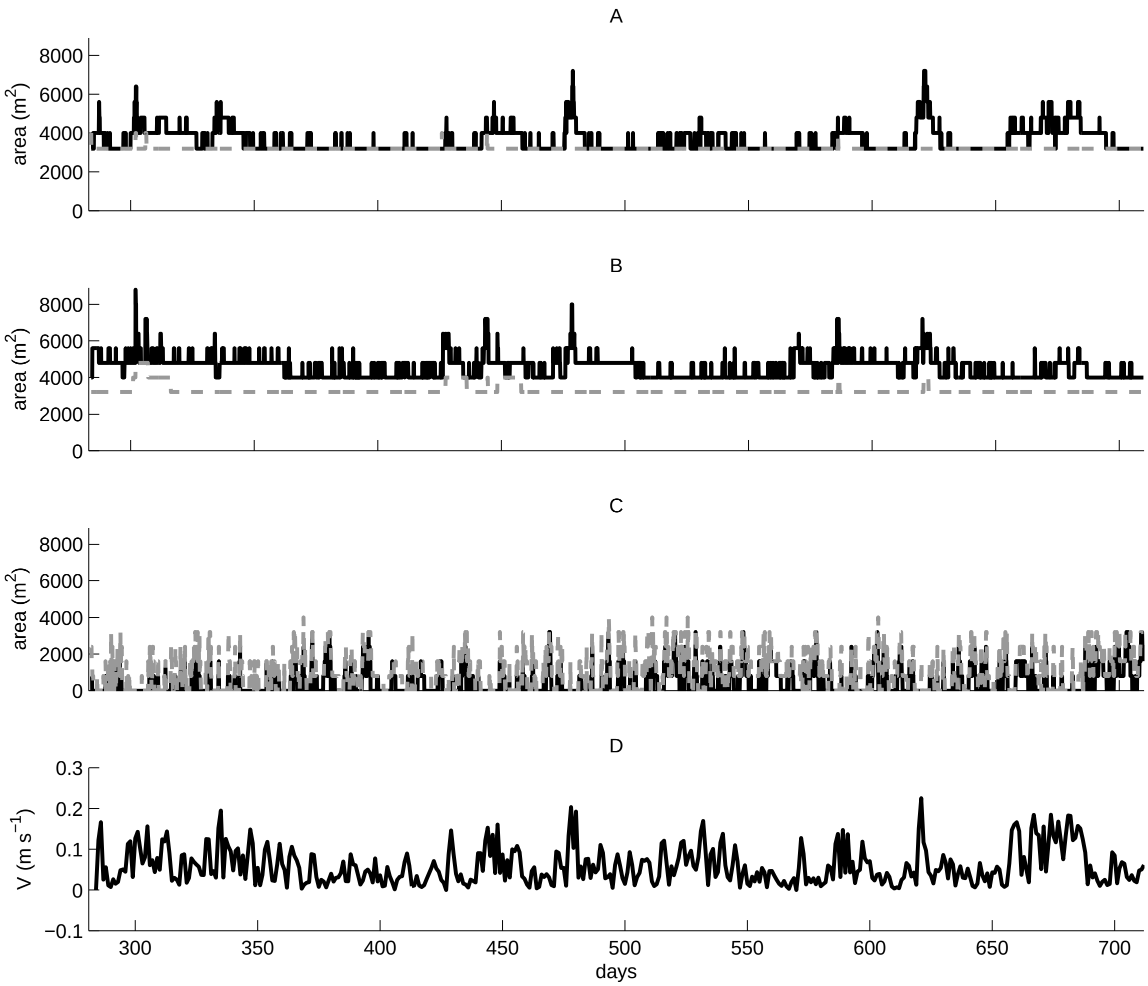
A
8000
6000
4000
2000
0
area (m^2)
B
8000
6000
4000
2000
0
area (m^2)
C
8000
6000
4000
2000
0
area (m^2)
D
0.3
0.2
0.1
0
−0.1
V (m s^{-1})
300
350
400
450
500
550
600
650
700
days

Figure 4:

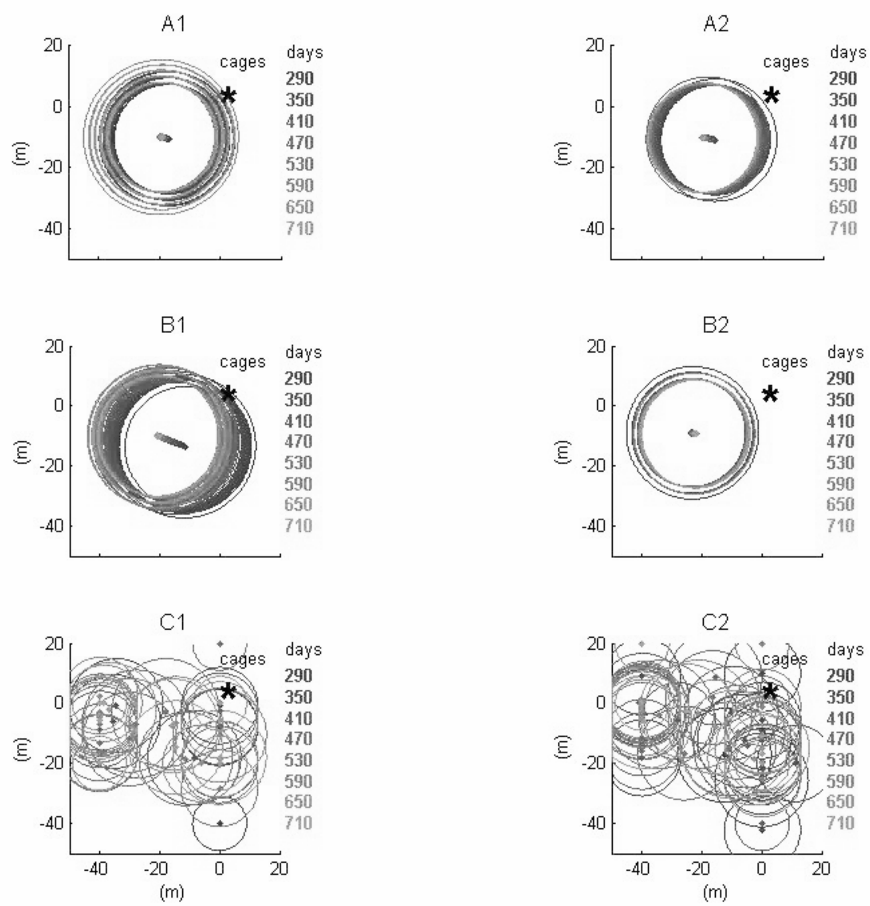

Figure 5:

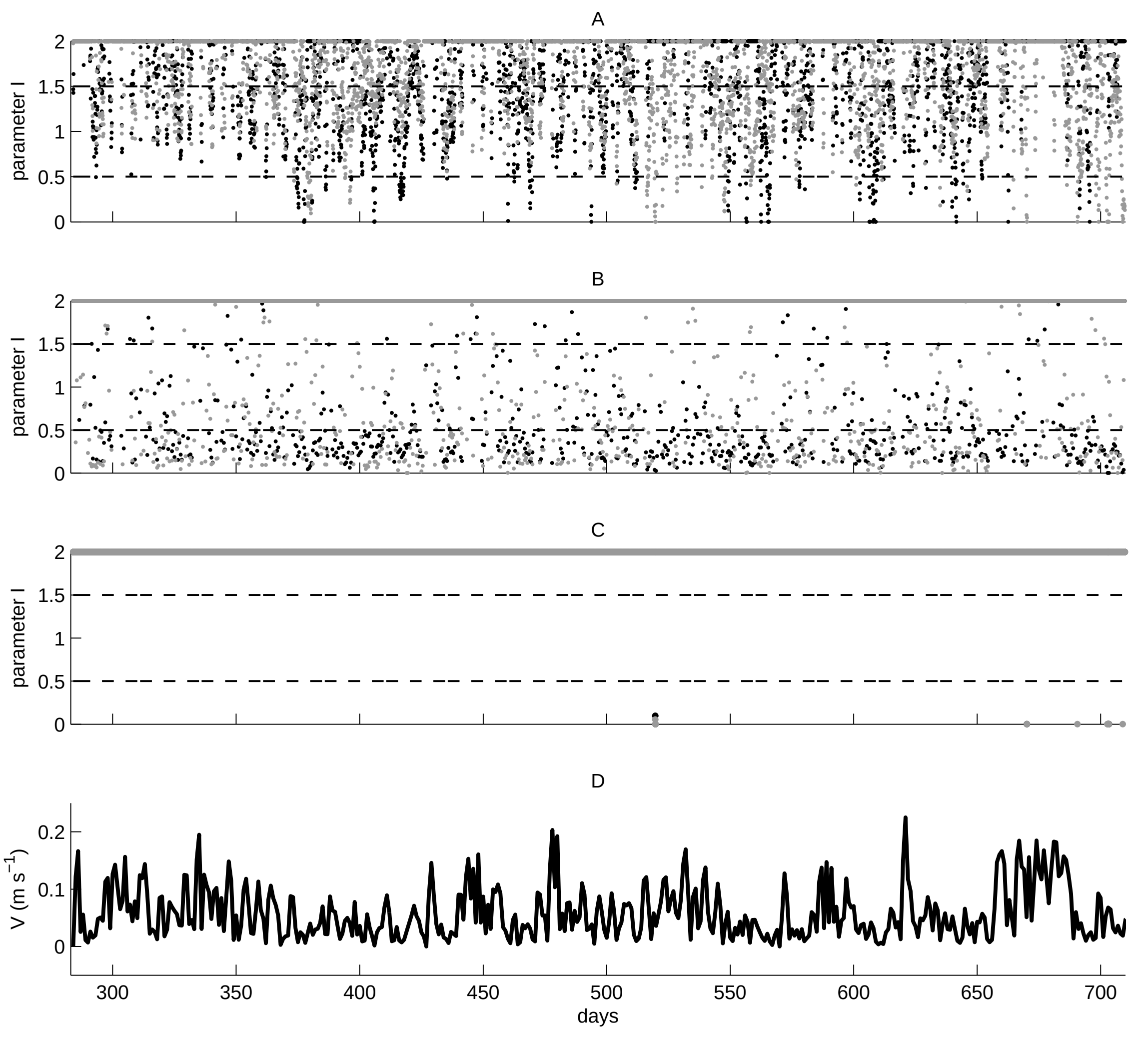
A
B
C
D
parameter I
V (m s^{-1})
days
0
0.5
1
1.5
2
0.1
0.2
300
350
400
450
500
550
600
650
700

Figure 6:

POM-LAMP3D parameters	value
POM physical domain (km)	46x16
LAMP3D physical domain (km)	8x4
Horizontal resolution (m)	400x200
Vertical resolution (m)	10
Barotropic cycle time step (s)	1
Smagorinsky diffusivity coefficient	0.1
Asselin filter coefficient	0.05
Ekman depth δ_{E} (m)	50
Wind drag coefficient C_{d}	0.001
Horizontal standard deviation $\boldsymbol{\sigma}$ (m)	3.46
Particle cycle time step (s)	60
Number of particles	620000
Feed conversion factor for organic carbon w^{C}_{feed} (mmolC particle^{-1})	308.6
Faeces conversion factor for organic carbon w^{C}_{faeces} (mmolC particle^{-1})	5.8
Feed conversion factor for nitrogen w^{N}_{feed} (mmolN particle^{-1})	167.8
Faeces conversion factor for nitrogen w^{N}_{faeces} (mmolN particle^{-1})	66.4
FOAM parameters	**value**
Physical domain (km)	8x4
Horizontal resolution (m)	40x20
O_2 supply parameter A (mmol$\mathrm{O_2}$ m^{-2} d^{-1})	736.3
O_2 supply parameter B (mmol$\mathrm{O_2}$ s m^{-3} d^{-1})	672.5
O_2 demand parameter C (mmol$\mathrm{O_2}$ mmolC^{-1})	1.07
O_2 demand parameter D (mmol$\mathrm{O_2}$ m^{-2} d^{-1})	-32.6
Settled matter non-stress N_s (mmolC m^{-2} d^{-1})	27.53
Settled matter intermediate-stress I_s (mmolC m^{-2} d^{-1})	57.50
Settled matter hyper-stress H_s (mmolC m^{-2} d^{-1})	30.59
I range amplitude parameter Δ_{fw}	0.5

Table 1:

Feed pellets		Faecal pellets	
Diameter (mm)	V_{sed} (m s^{-1})	Fish species [size (g)]	V_{sed} (m s^{-1})
3	0.087 $\downarrow$	*S. Aurata* [380]	0.004 $\downarrow$
3.5	0.118	*S. Aurata* [60]	0.005
4.5	0.103	*D. Labrax* [280]	0.006
5	0.144 $\Downarrow$	*D. Labrax* [80]	0.007 $\Downarrow$
6	0.088		

Table 2:

	Observations (m s^{-1})				
	Winter average (std)	Spring average (std)	Summer average (std)	Autumn average (std)	Annual average (std)
C1	0.066 (0.057)	0.075 (0.065)	0.063 (0.052)	0.070 (0.052)	0.069 (0.057)
	Model Output (m s^{-1})				
	Winter average (std)	Spring average (std)	Summer average (std)	Autumn average (std)	Overall average (std)
1st cycle	0.076 (0.051)	0.103 (0.084)	- -	- -	0.088 (0.047)
5th cycle	0.059 (0.034)	0.082 (0.066)	- -	- -	0.057 (0.034)
3th $\rightarrow$ 5th cycles	0.064 (0.042)	0.078 (0.050)	- -	- -	0.061 (0.034)

Table 3:

Exp.	**Simulation typology (release)**	***S*** **Impacted area mean ± std** (m^2)	**Parameter *I***			**Organic concentration mean ± std** ($gC\ m^{-2}$)
			no stress (% days)	**medium stress** (% days)	**high stress** (% days)	
A1	Slow feed (continuous)	3576 ± 582	74	22	4	1450 ± 404
A2	Quick feed (continuous)	3202 ± 41	71	27	2	1490 ± 453
B1	Slow feed (periodical)	4513 ± 563	87	4	9	895 ± 380
B2	Quick feed (periodical)	3277 ± 266	88	4	8	1590 ± 387
C1	Slow faeces	377 ± 656	99	0	1	< 1
C2	Quick faeces	941 ± 962	99	0	1	< 1

Table 4: